ESC European Society of Cardiology

Cardiovascular Research (2019) **115**, 1217–1227
doi:10.1093/cvr/cvz049

Protection against pressure overload-induced right heart failure by uncoupling protein 2 silencing

Azadeh Esfandiary[1†], Hanna S. Kutsche[2†], Rolf Schreckenberg[2], Martin Weber[2], Oleg Pak[1], Baktybek Kojonazarov[1], Akylbek Sydykov[1], Christine Hirschhäuser[2], Annemarie Wolf[2], Daniela Haag[1], Matthias Hecker[1], Ludger Fink[1], Werner Seeger[1], Hossein A. Ghofrani[1], Ralph T. Schermuly[1], Norbert Weißmann[1], Rainer Schulz[2], Susanne Rohrbach[2], Ling Li[2], Natascha Sommer[1‡], and Klaus-Dieter Schlüter[2*‡]

[1]Justus-Liebig-University Gießen, ECCPS, Aulweg 130, 35392 Gießen, Germany; and [2]Department of Physiology, Justus-Liebig University Gießen, Aulweg 129, 35392 Gießen, Germany

Received 24 October 2018; revised 31 January 2019; editorial decision 18 February 2019; accepted 6 March 2019; online publish-ahead-of-print 8 March 2019

Time for primary review: 20 days

Aims The role of uncoupling protein 2 (UCP2) in cardiac adaptation to pressure overload remains unclear. In a classical model of left ventricular pressure overload genetic deletion of UCP2 ($UCP2^{-/-}$) protected against cardiac hypertrophy and failure. However, in $UCP2^{-/-}$ mice increased proliferation of pulmonary arterial smooth muscle cells induces mild pulmonary hypertension, right ventricular (RV) hypertrophy, and reduced cardiac output. This suggests a different role for UCP2 in RV and left ventricular adaptation to pressure overload. To clarify this situation in more detail $UCP2^{-/-}$ and wild-type mice were exposed to pulmonary arterial banding (PAB).

Methods and results Mice were analysed (haemodynamics, morphometry, and echocardiography) 3 weeks after PAB or sham surgery. Myocytes and non-myocytes were isolated and analysed separately. Cell shortening of myocytes and fura-2 loading of cardiomyocytes were used to characterize their function. Brd assay was performed to study fibroblast proliferation. Isolated mitochondria were analysed to investigate the role of UCP2 for reactive oxygen species (ROS) production. UCP2 mRNA was 2.7-fold stronger expressed in RV myocytes than in left ventricular myocytes and stronger expressed in non-myocytes compared with myocytes. Three weeks after PAB, cardiac output was reduced in wild type but preserved in $UCP2^{-/-}$ mice. $UCP2^{-/-}$ had increased RV wall thickness, but lower RV internal diameters and displayed a significant stronger fibrosis. Cardiac fibroblasts from $UCP2^{-/-}$ had reduced proliferation rates but higher collagen-1 expression. Myocytes isolated from mice after PAB banding showed preserved function that was further improved by $UCP2^{-/-}$. Mitochondrial ROS production and respiration was similar between $UCP2^{-/-}$ or wild-type hearts.

Conclusion Despite a mild pulmonary hypertension in $UCP2^{-/-}$ mice, hearts from these mice are well preserved against additional pressure overload (severe pulmonary hypertension). This—at least in part—depends on different behaviour of non-myocytes (fibroblasts).

Keywords Pulmonary hypertension • Reactive oxygen species • Fibrosis • Cardiac remodelling • Cardiac protection

This article is part of the Spotlight Issue on Cardioprotection Beyond the Cardiomyocyte.

* Corresponding author. Tel: +49 641 99 47 212; fax: +49 641 99 19 729, E-mail: Klaus-Dieter.Schlueter@physiologie.med.uni-giessen.de

† The first two authors contributed equally to this study and share first authorship.

‡ The last two authors share senior authorship.

1. Introduction

Uncoupling proteins (UCP) represent a family of molecules that are located at the inner membrane of mitochondria. In mammalians, three main isoforms are expressed: UCP1, UCP2, and UCP3. While the role of UCP1, mainly located in the brown adipose tissue, is well known that of the two other isoform remains to be defined.[1,2] Based on the structural homology between the three isoforms, many researchers suggested a similar role as for UCP1 but the heterogenous distribution as well as functional measurements makes it unclear whether the three isoforms share common function.[3] Furthermore, the specific function of UCPs in different tissues may differ as well. UCP2 is constitutively expressed in the heart where it seems to be involved in fine tuning of cell metabolism as well as reactive oxygen species (ROS) defense.[4,5] The heart also expresses a second UCP isoform namely UCP3. The ratio between both isoforms in the heart may be different among species, but this is not well investigated.[6]

Of note, a recent study on cardiac stem cell differentiation suggested that UCP2 is mainly expressed during differentiation.[7] This would suggest that cardiac expression of UCP2 is strong in the foetal and neonatal heart and reduced in adulthood. In line with these assumptions, cardiac expression of UCP2 is induced during cardiac hypertrophy, i.e. in response to pressure overload.[8] The molecular adaptation of the heart to pressure overload is characterized by the re-expression of foetal type proteins, such as atrial natriuretic peptide, the β isoform of myosin heavy chain, or the B isoform of creatine kinase to mention just a few of them. Indeed, induction of UCP2 in the left ventricle (LV) upon heart failure has been reported.[9] Moreover, inhibition of UCP2 activity attenuates the transition of hypertrophy to heart failure.[10]

There is growing evidence that the LV and right ventricle differ in their ability to respond to pressure overload.[11] Although not properly worked out today, UCP2 may play a different role in both parts of the heart. We recently reported that UCP2$^{-/-}$ mice develop pulmonary hypertension, right heart hypertrophy, and a reduced cardiac output.[12] This may suggest that unlike earlier reports on the LV, UCP2 silencing will worsen the adaptation to pressure overload in the right heart. Therefore, the present study aimed to clarify the role of UCP2 for the response to an increase in right ventricular (RV) afterload. Unexpectedly, the data will show that non-myocytes play an important role in UCP2$^{-/-}$ mice during the adaptation to RV pressure overload.

2. Methods

2.1 Animals and ethic concerns

Adult male homozygous UCP2$^{-/-}$ mice (B6.129S4-Ucp2^{tm1Lowl}/J) were purchased from Jackson Laboratory (Bar Harbor, USA) and bred up to the 6th generation in our facility. Male C57BL/6J mice bought from Charles River Laboratories (Sulzfeld, Germany) were used as controls. All animal experiments conform to the guidelines from Directive 2010/63/EU of the European Parliament on the protection of animals used for scientific purposes. The experiments were registered under the numbers GI20/2010 Nr. 86/2011, GI 20/10 Nr. 40/2011, and GI 20/1 Nr. 91/2017.

2.2 Induction of an acute increase in RV afterload by pulmonary artery banding

Anaesthesia was initiated by isoflurane 3–4% and maintained by isoflurane 1.5–2.5% supplemented with 100% oxygen. Afterwards, mice were intubated and mechanically ventilated using a mouse ventilator MiniVent type 845 (Hugo Sachs Elektronik, March-Hugstetten, Germany), while placed on a heating surface. Analgesic buprenorphine hydrochloride (Temgesic®, 0.1 mg/kg, Sigma-Aldrich, Germany) was given subcutaneously. After left anterolateral thoracotomy via the second left intercostal space, a small titanium clip (Hemoclip®, Edward Weck& Co., Inc., Research Triangle Park, NC, USA) with a width of 0.35 mm was placed around the pulmonary trunk with a special hemoclip applier in order to produce 65–70% constriction of the pulmonary artery. The chest and afterwards the skin were closed with 6.0 prolene sutures. Sham operated mice underwent the same procedure without applying the hemoclip. In total, 18 wild type and 18 UCP2$^{-/-}$ mice were banded for this study. Mortality was 1/18 in wild-type mice and 0/18 in UCP2$^{-/-}$ mice.

2.3 Echocardiography

Vevo770 high-resolution imaging system equipped by 30-MHz transducer (VisualSonics, Toronto, Canada) was used to perform transthoracic echocardiography 3 weeks after operation. For *in vivo* heart function evaluation, the RV wall thickness (RVWT), RV internal diameter (RVID), tricuspid annular plane systolic excursion (TAPSE), and cardiac output (CO) were measured as described before.[13]

2.4 Invasive haemodynamic measurement

A series of pressure–volume loops was recorded with a micropressure conductance catheter (Millar instruments, Houston, USA). RV systolic pressure (RVSP) was measured through catheterization under anaesthesia 3 weeks after pulmonary arterial banding (PAB) or sham operation.

The animals were anaesthetized with 3–4% isoflurane supplemented with oxygen and ventilated with a rodent ventilator (Harvard Apparatus, Holiston, MA, USA). Maintenance of anaesthesia was done with 2–3% isoflurane supplemented with oxygen. The mice were laid supine on a heating platform with three legs taped to electrocardiogram electrodes for monitoring of heart rate. A rectal thermometer (Indus Instruments, Houston, TX, USA) was used to control the body temperature. The heating pad helped to keep the body temperature at 36.5–37.5°C .The right jugular vein was cannulated for measurement of RVSP.

2.5 Tissue sampling, RV hypertrophy assessment

Separation of RV wall from left ventricular wall and ventricular septum (S) was done. After heart hypertrophy measurements the RV wall, left ventricular wall, and S were fixed in formalin (3.5–3.7%), dehydrated and finally paraffin embedded for histological analysis. Collagen staining was performed by Picro Sirius Red staining. A total amount of 0.2 g Sirius Red was dissolved in 200 mL of picric acid, the solution was filtered and finally the pH was adjusted to pH 2.0. After staining the slices were measured using Leica QWin standard imaging software. Forty to 90 pictures were taken per ventricle and red stained collagen was normalized to the total tissue amount.

2.6 Isolation and culture of adult mouse ventricular cardiomyocytes

Ventricular cardiomyocytes were isolated from wild-type and UCP2$^{-/-}$ mice as described in detail elsewhere.[14] After deep anaesthesia with isoflurane (1.5–2.5%), hearts were excised from the chest cavity, transferred rapidly to ice-cold saline, and immediately mounted on the cannula of Langendorff perfusion system for isolation.

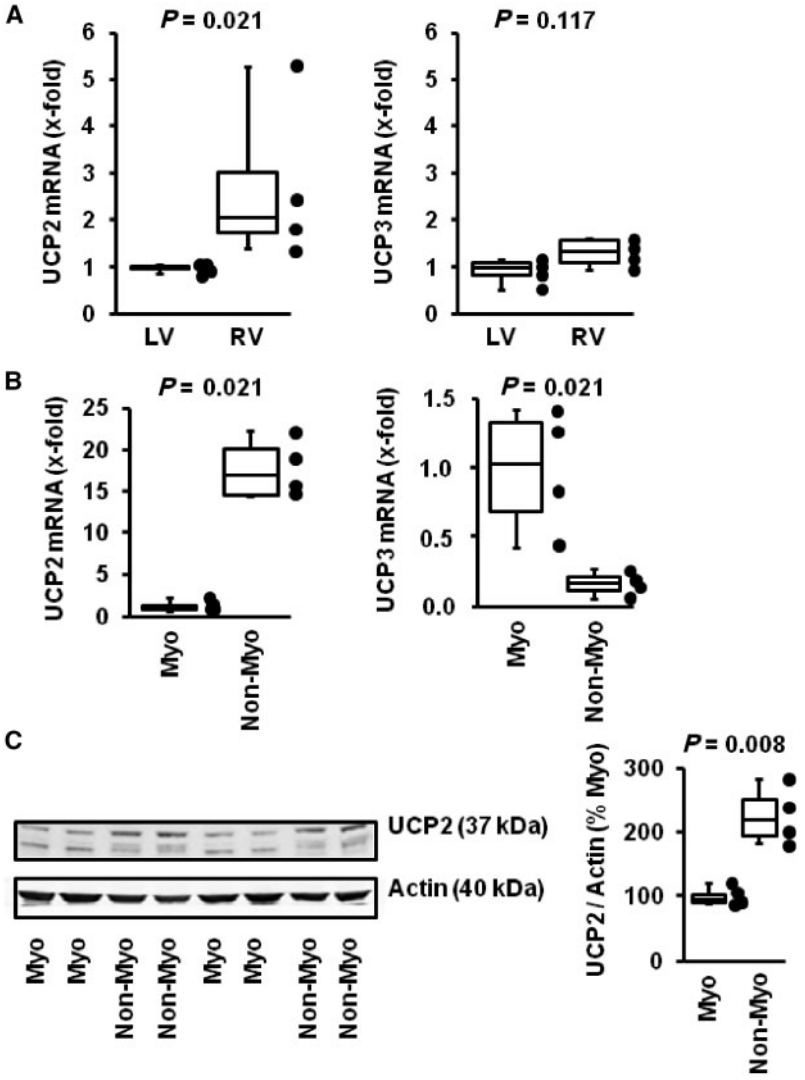

Figure 1 Distribution of UCP2 and UCP3 mRNA expression in left and right ventricle (*A*), myocytes and non-myocytes (*B*), and UCP2 protein expression in myocyes and non-myocytes (*C*). Data are from $n = 4$ mice and subsequent cell preparations and they are expressed as 25%, 50%, and 75% quartiles with whiskers representing the total range. The dots represent the individual data points. Data were analysed by a Shapiro–Wilk test to check whether data points are normally distributed and Levene test for equal variance. Subsequently, data were tested with an unpaired *t*-test. In *C* an original western blot is given with staining for UCP2 and actin.

2.7 Load-free cell shortening

Cell contraction determination was carried out at room temperature and analysed using a cell-edge-detection system as previously described.[15]

2.8 Calcium transient quantification

The fluorescent dye fura-2 AM was used to measure cytosolic calcium transients as described before.[16]

2.9 Cell spreading

Quantification of cell spreading (building of pseudopodia-like structures from cultured mice cardiomyocytes) was analysed by light microscopy as described before in detail.[17] Mouse myocytes were cultured in a modified medium containing the following additions: 20% foetal calf serum, mM: NaCl 118, KH_2PO_4 1.2, KCl 4.7, Glucose 5, $MgSO_4$ 0.8, HEPES 10, $CaCl_2$ 2.5, and pyruvate 1.9, gassed with carbogen. The pH was adjusted to 7.4.

2.10 RNA isolation and real-time PCR

Total RNA was extracted from RV and LV by RNeasy Micro Kit (Qiagen N.V., Hilden, Germany) and the extracted mRNA was reverse-transcribed to cDNA using the iScript cDNA Synthesis Kit (Bio-Rad, Berkeley, CA, USA). The mRNA expression of UCP2 and UCP3 was quantified by master mix for RT PCR (iTaq SYBR Green supermix withROX, Bio-Rad, Berkeley, CA, USA) and Mx3000P QPCR Systems (AgilentTechnologies, Santa Clara, USA). Primer efficiency for UCP2 and UCP3 was 78% and 79%, respectively. Hypoxanthine phosphoribosyltransferase (HPRT) was used as housekeeping gene. The used reaction condition was 1× (95°C, 10 min) followed by 45× (95°C, 5 s; 60°C, 5 s, 72°C, 10 s) and the extension phase was done at 72°C. Measurement of

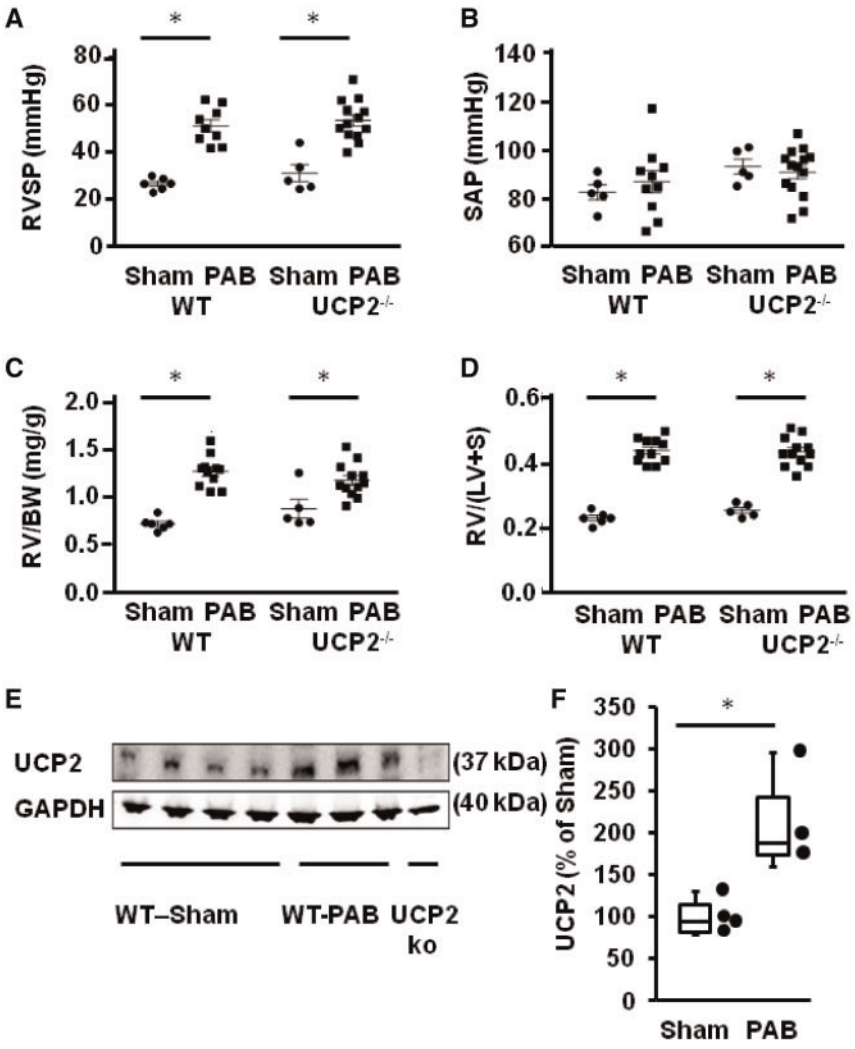

Figure 2 Pressure overload, hypertrophy, and UCP2 expression in mice 3 weeks after pulmonary artery banding (PAB; $n = 14$ wild type; $n = 14$ UCP2$^{-/-}$) or sham surgery ($n = 8$ wild type; $n = 15$ UCP2$^{-/-}$). (*A*) Right ventricular systolic pressure (RVSP in mmHg), (*B*) systemic arterial pressure (SAP, in mmHg), (*C*) right ventricular weight normalized to body weight (RV/BW, in mg/g), and (*D*) right ventricular weight normalized to the left ventricle and septum weight [RV/(LV + S)]. Data are given for sham surgery and PAB banding of each genotype. A one-way ANOVA with a subsequent Student–Newman–Keuls test for *post hoc* analysis was performed. Normal distribution was tested with a Shapiro–Wilk test. (*E*) Original blot of RV samples from wild-type mice 3 weeks after banding (PAB; lane 5–7), sham (lane 1–4), or UCP$^{-/-}$ mice (lane 8). (*F*) Quantification of UCP2 expression (after normalization to GAPDH). Data are expressed as % of sham ($n = 3$–4 as indicated in *E*). They are expressed as 25%, 50%, and 75% quartiles with whiskers representing the total range. Data in *F* were analysed by a Shapiro–Wilk test to check whether data points are normally distributed and Levene test for equal variance. Subsequently, data were tested with an unpaired *t*-test. *P<0.05.

each gene was carried out as duplicate. Confirmation of the desired products formation was done by dissociation curves. The calculation of ΔC_t values was done by subtracting the C_t values of the target gene from the endogenous control [ΔC_t = C_t (endogenous control) - C_t (target)], and the fold change according $2^{\Delta\Delta}$Ct formula was calculated.

2.11 Proliferation assay

The non-myocyte fraction of the isolated cells was used to separate cardiac fibroblasts. Non-myocytes were placed on a culture dish and the dishes were washed after 30 min to eliminate non-attached cells (mainly endothelial cells). Proliferation was quantified by bromo-uridine incorporation. Cells were lysed after 12 and 48 h and stained with a fluorescence antibody. Quantification was subsequently performed via ELISA (5-Bromo-2′-deoxy-uridine Labeling and Detection Kit I; Merck, Darmstadt, Germany).

2.12 Western blot

Western blots were performed with protein samples as indicated. After transfer to a nitrocellulose membrane samples were incubated with either an antibody directed against UCP2 and subsequently with an antibody directed against actin or voltage-dependent anion exchanger (VDAC) or GAPDH. Signals were detected by a fluorescence coupled secondary antibody (Abcam, ab6940). Western blots dealing with UCP2 expression were performed with an antibody evaluated before.[18]

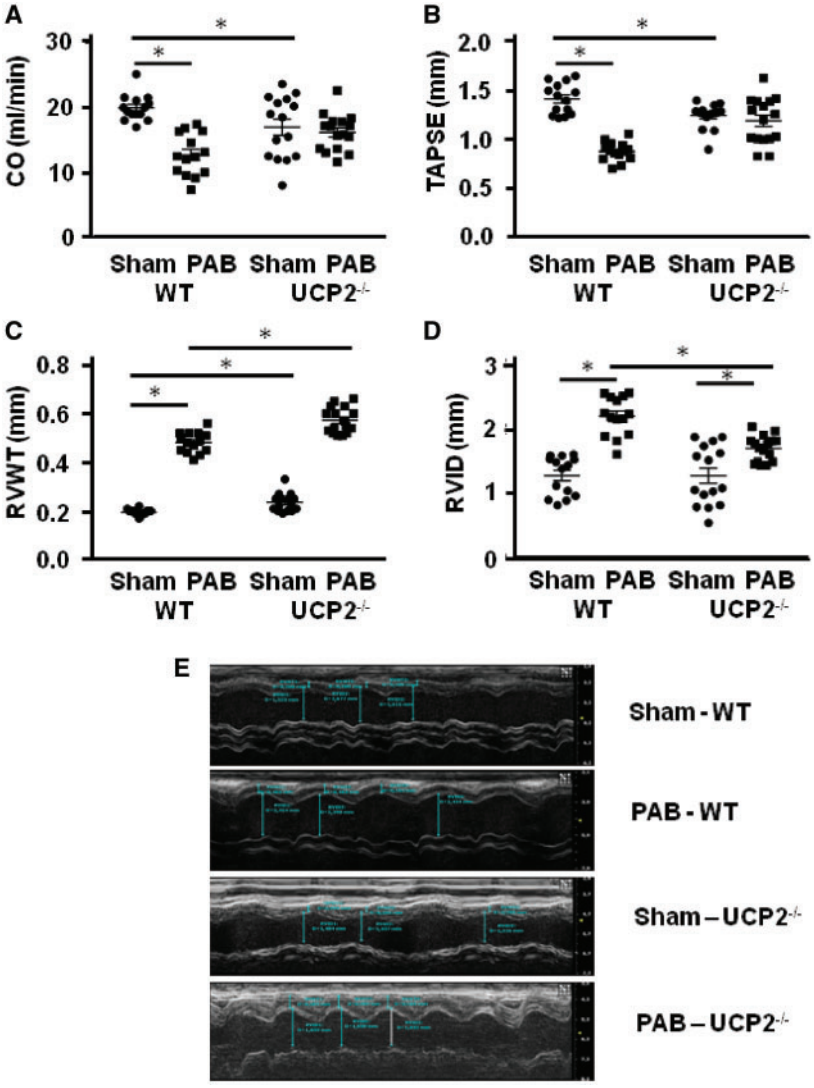

Figure 3 Cardiac function in mice 3 weeks after pulmonary artery banding (PAB). (*A*) Cardiac output (CO, in mL/min), (*B*) tricuspid annular plane systolic excursion (TAPSE, in mm); (*C*) right ventricular wall thickness (RVWT, in mm), (*D*) right ventricular internal diameter (RVID, in mm), and (*E*) representative images of echo analysis. Data are given for sham surgery and PAB banding of each genotype. A one-way ANOVA with a subsequent Student–Newman–Keuls test for *post hoc* analysis was performed. Normal distribution was tested with a Shapiro–Wilk test. The number of mice in the individual groups corresponds to *Figure 2A–D*. *$P<0.05$.

Specificity was tested in tissue samples from spleens of $UCP2^{-/-}$ mice and wild-type mice, respectively (Supplementary material online, *Figure S1*). Control peptide for UCP2 was a recombinant human UCP2.[19]

2.13 Amplex ultra red measurements of mitochondria

The isolation of cardiac mitochondria from mice hearts has been described before.[20,21]

2.14 Statistical analysis

Data were expressed as boxes representing the 25%, 50%, and 75% quartile with whiskers indicating the range of all data. Where indicated data were plotted as individual spots of individual data points with means ± SEM in addition. Statistical analysis was performed using SPSS22.0. The different experimental groups were statistically analysed by one-way ANOVA and Newman–Keuls *post hoc* test for multiple comparisons. *P*-values of <0.05 were considered as statistically significant.

3. Results

3.1 Expression of UCP2/3 in mouse hearts

At first, we investigated the mRNA expression of UCP2 and UCP3 in mouse hearts. In the right ventricle, UCP2 mRNA expression was nearly double of that measured in the LV. However, expression of UCP3 did not differ between both ventricles (*Figure 1A*). Next, we investigated the expression between myocytes and non-myocytes. To reach this aim we isolated ventricular myocytes and separated them from the non-myocytes of the right ventricle. The data show that UCP2 mRNA is constitutively expressed in both cell preparations but much stronger in non-myocytes, whereas

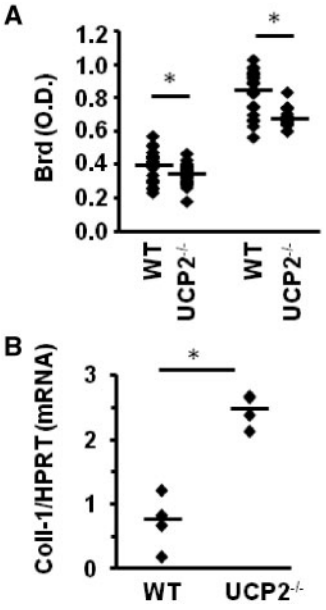

Figure 4 Analysis of cardiac fibroblasts *in vitro*. (*A*) Proliferation of fibroblasts isolated from wild-type mice (WT) or UCP2$^{-/-}$ mice was quantified by Brd-incorporation and subsequent determination of optical densities (O.D.) in the cultures dishes. Data are from $n = 24$ samples each (six mice). (*B*) Quantification of collagen-1 mRNA expression in isolated fibroblasts from WT and UCP2$^{-/-}$ mice ($n = 4$ each). Data were analysed by a Shapiro–Wilk test to check whether data points are normally distributed and Levene test for equal variance. Subsequently, data were tested with an unpaired *t*-test. *$P<0.05$.

UCP3 is predominantly expressed in myocytes and only to a minor proportion in non-myocytes (*Figure 1B*). We confirmed these data using a UCP2 specific antibody. As indicated in the representative western blot (*Figure 1C*) UCP2 protein is stronger expressed in the non-myocyte fraction than in the myocyte fraction. Data are normalized to actin expression.

3.2 Effect of PAB on RV hypertrophy

PAB was performed on wild-type and UCP2$^{-/-}$ mice to clarify the role of UCP2 in the RV adaptation to pressure overload. As expected, RV pressure increased in mice under PAB but systemic blood pressure remained constant (*Figure 2A* and *B*). There were no differences between both mouse strains. Similarly, RV hypertrophy normalized to body weight (*Figure 2C*) or left ventricle and septum (*Figure 2D*) increased under PAB but without any differences between both strains. Furthermore, 3 weeks after surgery, RV expression of UCP2 was increased (*Figure 2E* and *F*). However, cardiac output decreased in wild-type mice 3 weeks after PAB but remained stable in UCP2$^{-/-}$ mice (*Figure 3A*). Similarly, TAPSE—a standard parameter of RV diastolic function—remained stable in UCP2$^{-/-}$ mice but was reduced in wild-type mice (*Figure 3B*). RVWT increased more stronger in UCP2$^{-/-}$ in comparison to wild-type mice under PAB (*Figure 3C*), whereas RV internal diameter remained smaller (*Figure 3D*). Representative figures are given in *Figure 3E*. Collectively, the data support the picture of mal-adaptive type of hypertrophy in wild-type mice but adaptive RV hypertrophy in UCP2$^{-/-}$ mice.

3.3 Fibrosis and cardiac fibroblasts with UCP2 deficiency

In mice hearts non-myocytes express more UCP2 than myocytes (*Figure 1B* and *C*). Therefore, we were first interested to investigate the effect of UCP2 deficiency in cardiac fibroblasts. We observed two genotype-specific differences in the behaviour of cultured cardiac fibroblasts between wild-type and UCP2$^{-/-}$ mice. First, proliferation of fibroblasts isolated from UCP2$^{-/-}$ was less than that of fibroblasts isolated from wild-type mice (*Figure 4A*). Second, fibroblasts from UCP2$^{-/-}$ mice displayed a higher endogenous expression of collagen-1 mRNA (*Figure 4B*). These *in vitro* data let us speculate that fibroblasts from both genotypes react different during the RV adaptation to pressure overload. Indeed, collagen content was increased in the PAB mice and significantly more elevated in UCP2$^{-/-}$ mice (*Figure 5A* and *B*). Thus, non-myocytes from wild-type mice express a large amount of UCP2 and depletion of UCP2 leads to a more differentiated cell phenotype allowing the generation of more extracellular matrix upon mechanical overload of the right ventricle.

3.4 Function of myocytes with UCP2$^{-/-}$

The aforementioned experiments on fibrosis support the suggestion that cardiac fibroblasts are involved in the RV adaptation of UCP2$^{-/-}$ hearts to pressure overload. Next, we investigated whether additional differences occur for myocytes as well. RV myocytes from both strains were isolated from sham or PAB mice 3 weeks after onset of pressure overload and the load-free cell shortening was analysed. Myocytes isolated from the right ventricle of wild-type mice after PAB showed an improved load-free cell shortening, maximal contraction velocity, and maximal relaxation velocity when compared with those isolated from sham operated mice (*Figure 6A*). Similarly, myocytes isolated from UCP2$^{-/-}$ had an improved function (*Figure 6A*). In a second series of experiments calcium transients were quantified by fura-2 fluorescence. Here, myocytes from UCP2$^{-/-}$ had greater calcium transients compared with wild-type myocytes under PAB and greater time to basal calcium levels than myocytes from sham wild-type mice (*Figure 6B*). In conclusion, cardiomyocytes from wild type and UCP2$^{-/-}$ do not develop intrinsic failure within 3 weeks of PAB. Next, we analysed the ability of myocytes to adapt to culture conditions. Myocytes isolated from a three-dimensional tissue have to adapt to the two-dimensional surface of culture dishes. This process mimics some of the aspects required to cardiac adaptation and can be monitored by the formation of pseudopodia-like structures a process known as spreading (*Figure 7A*). Myocytes from both strains showed a rapid adaptation (*Figure 7B*) with no differences among strains (*Figure 7C*).

3.5 UCP2$^{-/-}$ and ROS

Currently, the precise function of UCP2 in cardiac cells is not clear. There are suggestions that UCP2 may modify the amount of ROS produced within the electron transport chain but current data are inconclusive. To clarify the point whether UCP2 modifies basal mitochondrial function, we first verified its expression in mitochondria. As indicated in the representative western blot shown in Supplementary material online, *Figure S1A*, UCP2 is constitutively expressed in subsarcolemmal and interfibrillar mitochondria. Purification was verified by co-staining with VDAC and specificity of the antibody by co-staining with a control peptide and whole tissue samples from the spleen of wild-type and UCP2$^{-/-}$ mice. Spleen is the tissue with the highest expression of UCP2. Respiration rate was not different between mitochondria isolated from wild-type and UCP2$^{-/-}$ mice. This holds for complex I and complex II

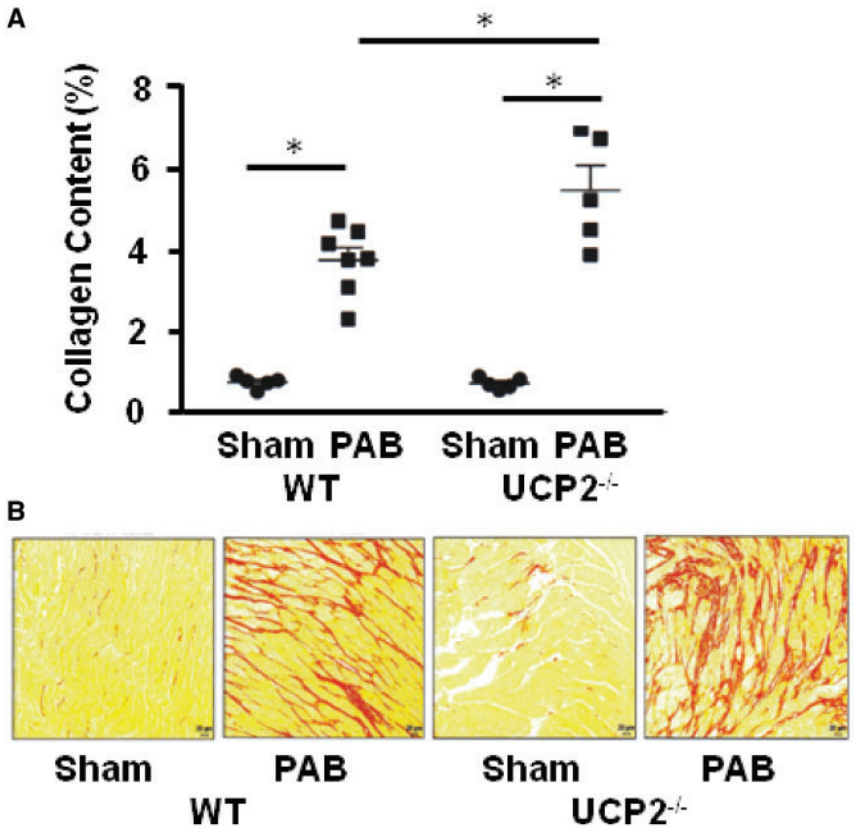

Figure 5 Right ventricular fibrosis in mice 3 weeks after pulmonary artery banding (PAB). (*A*) Collagen staining quantified as percent PircoSirius Red staining. Data are from $n = 7$ mice (sham, wild type), $n = 7$ mice (PAB wild type); $n = 5$ (sham UCP2$^{-/-}$), and $n = 5$ (PAB UCP2$^{-/-}$). (*B*) Representative images. Data are given for sham surgery and PAB banding of each genotype. A one-way ANOVA with a subsequent Student–Newman–Keuls test for *post hoc* analysis was performed. Normal distribution was tested with a Shapiro–Wilk test. *$P<0.05$.

substrates under basal and ADP-dependent forced respiration (supplementaryentary material online, *Figure S1B*). In isolated mitochondria from wild type and UCP2$^{-/-}$ mice ROS formation did also not differ between mitochondria from both genotypes (Supplementary material online, *Figure S2*), neither at baseline nor during ADP administration; in accordance with these findings, in isolated mitochondria application of genipin—a pharmacological UCP inhibitor—did not affect ROS formation either (Supplementary material online, *Figure S2*).

4. Discussion

The main finding of our study is that UCP2 deficiency attenuates a loss of RV function upon pressure overload as quantified by cardiac output. Our data suggest that cardiac fibroblasts are mainly responsible for this finding. This conclusion is based on the following results that were obtained in our study: First, in mice hearts non-myocytes express significantly more UCP2 than myocytes. Secondly, deficiency of UCP2 leads to alterations in fibroblast proliferation and collagen expression. Third, under pressure overload right ventricle in UCP2$^{-/-}$ mice produced more collagen than the right ventricle in wild-type mice. Fourth, in contrast to fibroblasts and collagen production, no major functional differences were observed between myocytes isolated from both strains when analysed 3 weeks after PAB. In summary, these genotype-specific differences lead to preserved right heart function in UCP2$^{-/-}$ mice.

Adaption of cardiac tissue to pressure overload is characterized by reinduction of foetal-type proteins such as atrial natriuretic peptide, the β isoform of myosin heavy chain, and the B-type isoform of creatine kinase to name just a few of them. UCP2 induction in cardiac hypertrophy might be another example for this rule. It is generally assumed that pressure overload leads to an induction of UCP2 supporting the idea that UCP2 participates in the transition of myocardial hypertrophy to heart failure.[8–10] It is in line with these assumptions that UCP2 expression is high in differentiating myocytes and declines later in terminal differentiated myocytes.[7,22] Looking carefully in the literature, data suggest even no expression of UCP2 in the heart or stable expression of UCP2 mRNA.[8,23] Here, we found a significant increase in right ventricle UCP2 protein expression 3 weeks after PAB. Conflicting data about the expression of UCP2 in heart tissue may come from specificity of antibodies. Specificity of the antibody used here was carefully confirmed. It shows that a protein band was detected that is in the right molecular size (see control peptide, a recombinant human UCP2 peptide) and that the antibody detects a protein band in the spleen from wild-type mice but not from UCP2$^{-/-}$ mice. The antibody was previously characterized.[18] Therefore, we have strong evidence that UCP2 expression is induced in response to pressure overload of the right ventricle.

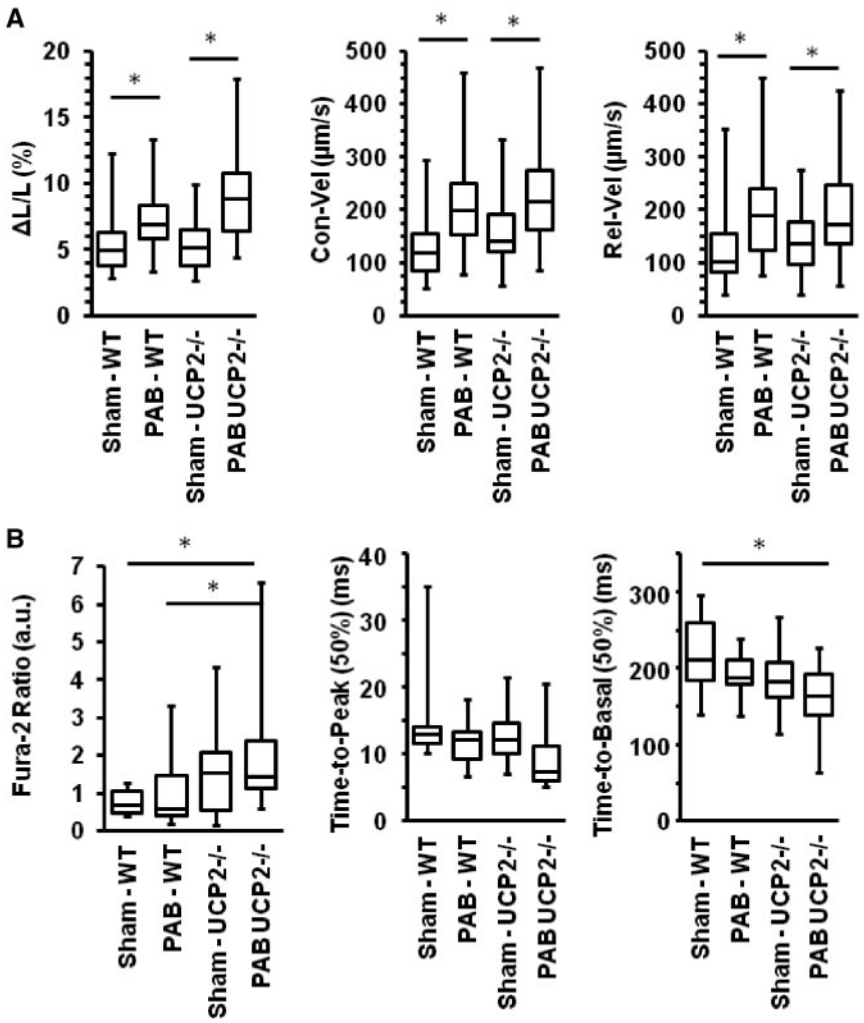

Figure 6 Cell shortening and calcium transients of isolated right ventricular myocytes. (*A*) Data show the normalized cell shortening (ΔL/L, %), maximal contraction velocity (Con-Vel, µm/s), and the maximal relaxation velocity (Rel-Max, µm/s). Data are from $n = 90$ to 122 cells (eight mice) and they are expressed as 25%, 50%, and 75% quartiles with whiskers representing the total range. (*B*) Data show the amplitude of calcium transients (Fura-2 ratio), of the time to reach 50% of the maximal peak (Time-to-Peak 50%), and the time to reach 50% of the basal level of intracellular calcium (Time-to-Basal 50%). Data are from $n = 18$ to 26 cells and they are expressed as 25%, 50%, and 75% quartiles with whiskers representing the total range. A one-way ANOVA with a subsequent Student–Newman–Keuls test for *post hoc* analysis was performed. Normal distribution was tested with a Shapiro–Wilk test. *$P<0.05$.

UCP2 has been described as an UCP and may affect respiration and ROS formation in mitochondria. However, our own experiments do not support such a role for UCP2 in cardiac mitochondria. Alternatively, silencing of UCP2 may favour the use of glucose by cells. Furthermore, silencing of UCP2 in pancreatic adenocarcinoma cells activated the Akt/mTOR pathway that is normally linked to cell proliferation.[24] Pulmonary artery smooth muscle cells show an accelerated proliferation rate under UCP2 silencing as well.[12] Thus, there are alternative pathways by which UCP2 may affect cell behaviour. Our experiments with isolated fibroblasts show that UCP2 modifies fibroblast activity. Fibroblasts isolated from $UCP2^{-/-}$ mice showed less proliferation but more collagen-1 mRNA expression suggesting a more differentiated cell phenotype. These data suggest that the increased fibrosis in hearts from $UCP2^{-/-}$ under PAB may be based on direct fibroblast activation.

Reactive fibrosis is an interstitial deposition of collagens surrounding cardiomyocytes and perivascular areas,[25,26] while replacement fibrosis develops following cardiomyocyte damage and is evident if cardiomyocyte loss occurs.[26] RV myocardial stiffness is increased with mild and severe RV dysfunction. While in mild RV dysfunction (fibrosis in between 5% and 10%) stiffness is mainly determined by increased myofibril stiffness[27] in severe RV dysfunction (fibrosis >10%), both myofibril- and fibrosis-mediated stiffness contribute to increased RV myocardial stiffness.[27,28] Based on these assumptions a massive RV fibrosis may increase RV stiffness that then contributes to functional impairment[28]. However, a certain level of fibrosis might be beneficial because it provides mechanical support to cardiomyocytes surrounding and prevents excessive RV dilation and deformation due to pressure overload.[29,30] Indeed, in patients with severe RV pressure overload often less than 10% of ventricular volume is fibrosis and fibrosis is often limited to the RV septal insertion points. These patients may also display severe RV failure their ventricular function recovers after lung transplantation (for review, see ref.[29]).

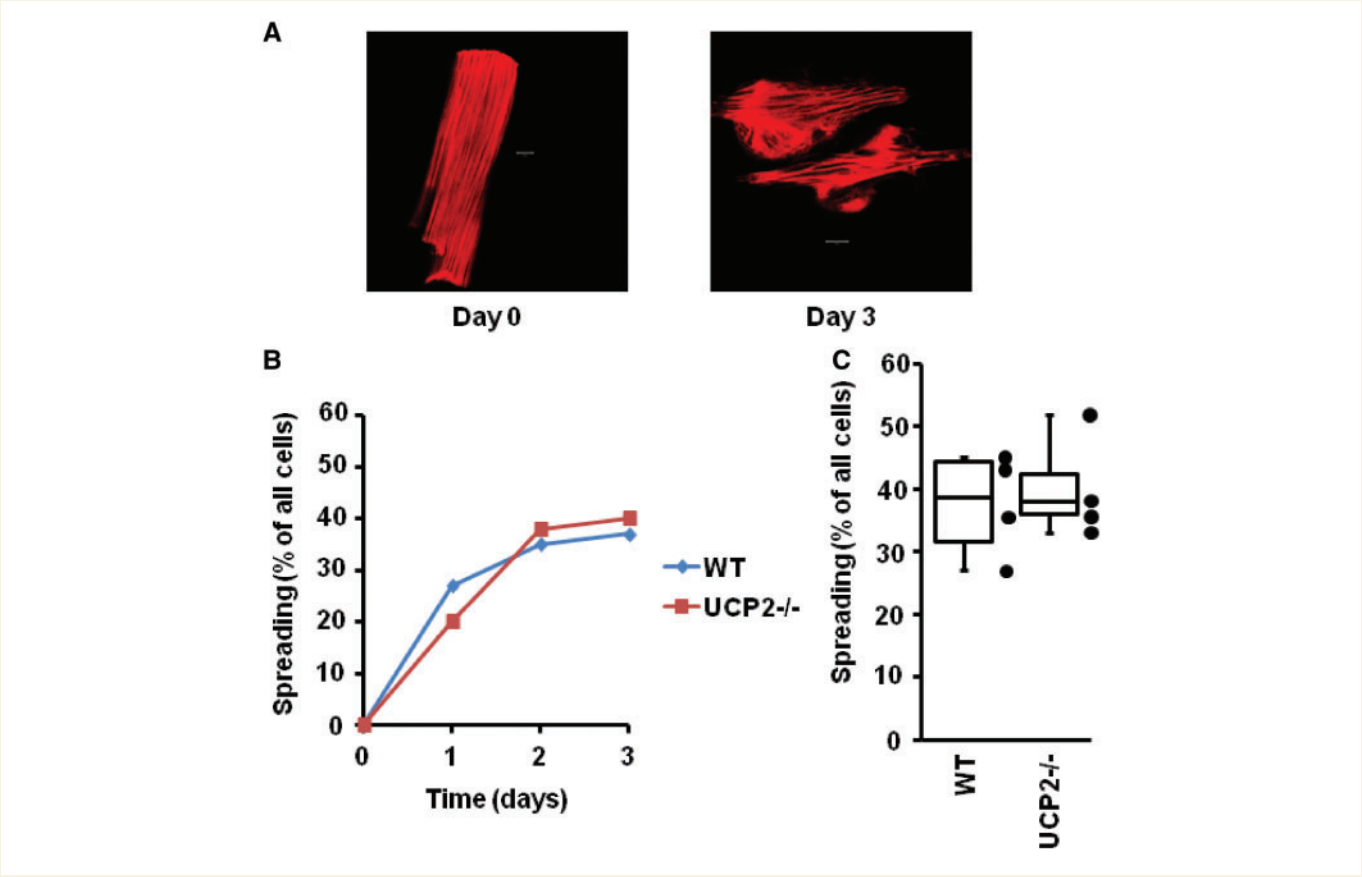

Figure 7 Cellular adaptation to culture conditions. (*A*) The phalloidin-TRITC stained myocytes indicate the native shape (Day 0) and the adaptation by performing pseudopodia-like structures (spreading, Day 3). (*B*) Representative time relationship of the ability of mouse myocytes to adapt to the culture dish by spreading. (*C*) Quantitative analysis of the percent of cells that respond to cultivation by spreading. Data are from $n = 4$ preparations/mice each and they are expressed as 25%, 50%, and 75% quartiles with whiskers representing the total range. Data in *C* were analysed by a Shapiro–Wilk test to check whether data points are normally distributed and Levene test for equal variance. Subsequently, data were tested with an unpaired *t*-test ($P > 0.05$).

In accordance with these studies, in the present study RV internal diameter was lower in UCP2$^{-/-}$ mice compared with wild-type mice and RVWT is increased. As a consequence pulmonary hypertension left–right asynchrony occurs, cardiac oxygen delivery and energy metabolism changes, and neurohumoral activation is observed. All these alterations contribute to the loss of pump function,[31] and a better adaptation in UCP2$^{-/-}$ mice compared with wild-type mice helps to preserve cardiac output. The different responsiveness of UCP2-deficient fibroblasts may support this better adaptation.

Besides their contribution to changes in mechanical properties of the tissue, fibroblasts can actively influence cardiomyocyte function by release of paracrine factors contributing to hypertrophy.[32] In rats, RV hypertrophy due to pulmonary artery banding is associated with increased RV contractility as assessed by the slope of the end-systolic pressure–volume relationship (EES), although RV failure with decreased ejection fraction and cardiac output is measured.[33] Our study confirmed these findings on EES in mice as isolated cardiomyocytes were not functionally depressed.

Whether, there exists a 'threshold' level of RV fibrosis, above which the fibrosis becomes detrimental and drives RV failure, is not clear. The correlation between increased fibrosis on the one hand and stabilized function on the other hand was not expected. However, pressure overload requires increased force production from myocytes but this needs to be transferred to the extracellular matrix. In the light of the functional outcome of the *in vivo* part of our study the data suggest that the increase in fibrosis is insufficient in wild-type mice and that the heart benefits from a slightly stronger fibrosis as given in UCP2$^{-/-}$ mice. In line with these assumptions, we could not detect any malfunction on the cellular level of myocytes isolated from wild-type mice or UCP2$^{-/-}$ mice. The only statistical significant difference in myocytes between both genotypes was an accelerated rate of restoration of intracellular calcium levels during the diastolic phase in myocytes from UCP2$^{-/-}$. This suggests an improved SERCA activity leading to higher calcium transients as we could indeed measure. Previously, over-expression of UCP2 in cardiomyocytes was shown to have the opposite.[34] We could not observe any indication for reduced SERCA activity in myocytes isolated from wild-type mice, in accordance with previous data with a mild form of PAB in a canine model.[35] Load-free cell shortening as the sum of calcium transients and intrinsic elastic performance of myocytes was not different between myocytes isolated from both strains. Therefore, differences between myocytes from both strains seem not to be the dominant effect to explain the strong difference in cardiac output between them. Despite the preserved RV function under pressure overload in UCP2$^{-/-}$ but not wild-type mice, cardiac output and TAPSE were slightly lower in UCP2$^{-/-}$ mice compared with wild-type mice confirming an earlier study.[12] The reason for this difference remains unclear but the results from the present study rule out that

cardiomyocytes *per se* have an impaired function. In the previous study, the authors argued that the lower basal RV functions in UCP2$^{-/-}$ mice are responsible for the small increase in pulmonary artery pressure despite vascular remodelling. This would, again, be mainly confirmed by non-myocytes due to our additional experiments in the present study.

5. Conclusion

UCP2 deficiency in mice significantly preserves the right heart function under pressure overload. This is associated with a stronger fibrosis. It should be pointed out that mice cardiac fibroblasts express more UCP2 than myocytes and that UCP2 is by far the most dominant UCP isoform in this cell type. Since cardiomyocytes function was preserved in wild-type and UCP2$^{-/-}$ mice during pressure overload, the increased fibrosis might contribute to the preservation of right heart function during pulmonary artery banding in UCP2$^{-/-}$ mice.

Supplementary material

Supplementary material is available at *Cardiovascular Research* online.

Acknowledgements

We thank Nadine Woitasky, Daniela Schreiber, and Peter Volk for excellent technical support. We thank Elena Pohl (Department of Biomedical Science, University of Veterinary Medicine, Vienna, Austria) for providing us a suitable UCP2 antibody and recombinant hUCP2.

Conflict of interest: none declared.

Funding

This study was supported by the Deutsche Forschungsgemeinschaft (DFG). The study (A06 and B05) is part of the collaborative research centre 1213.

References

1. Azzu V, Jastroch M, Divakaruni AS, Brand MB. The regulation and turnover of mitochondrial uncoupling proteins. *Biochim Biophys Acta* 2010;**1797**:785–791.
2. Esteves TC, Brand MD. The reactions catalysed by the mitochondrial uncoupling proteins UCP2 and UCP3. *Biochim Biophys Acta* 2005;**1709**:35–44.
3. Mattiasson G, Sullivan PG. The emerging functions of UCP2 in health, disease, and therapeutics. *Antioxid Redox Signal* 2006;**8**:2–22.
4. Ruiz-Ramirez A, Lopez-Acosta O, Barrios-Maya MA, El-Hafidi M. Cell death and heart failure in obesity: role of uncoupling proteins. *Oxid Med Cell Longev* 2016;**2016**:9340654
5. Ježek P, Holendová B, Garlid KD, Jabůrek M. Mitochondrial uncoupling proteins: subtle regulators of cellular redox signaling. *Antioxid Redox Signal* 2018;**29**:667–714.
6. Alan L, Smolkova K, Kronusova E, Santorova J, Jezek P. Absolute levels of transcripts for mitochondrial uncoupling proteins UCP2, UCP3, UCP4, and UCP5 show different patterns in rat and mice tissues. *J Bioenerg Biomembr* 2009;**1**:71–78.
7. Hilse KE, Rupprecht A, Egerbacher M, Bardakji S, Zimmermann L, Wulczyn AEM, Pohl EE. The expression of uncoupling protein 3 coincides with the fatty acid oxidation type of metabolism in adult murine heart. *Front Physiol* 2018;**9**:747.
8. Fukunaga Y, Itoh H, Hosoda K, Doi K, Matsuda J, Son C, Yamashita J, Chun T-H, Tanaka T, Inoue M, Masatsugu K, Saito T, Sawada N, Nakao K. Altered gene expression of uncoupling protein-2 and -3 in stroke-prone spontaneously hypertensive rats. *J Hypertension* 2000;**18**:1233–1238.
9. Huntgeburth M, Tiemann K, Shahverdyan R, Schlüter KD, Schreckenberg R, Gross ML, Mödersheim S, Caglayan E, Müller-Ehmsen J, Ghanem A, Vantler M, Zimmermann WH, Böhm M, Rosenkranz S. Transforming growth factor β_1 oppositely regulates the hypertrophic and contractile response to β-adrenergic stimulation in the heart. *PLos One* 2011;**6**:e26628.
10. Ji XB, Li XR, Hao-Ding, Sun Q, Zhou Y, Wen P, Dai CS, Yang JW. Inhibition of uncoupling protein 2 attenuates cardiac hypertrophy induced by transverse aortic constriction in mice. *Cell Physiol Biochem* 2015;**36**:1688–1698.
11. Schreckenberg R, Rebelo M, Deten A, Weber M, Rohrbach S, Pipicz M, Csonka C, Ferdinandy P, Schulz R, Schlüter K-D. Specific mechanisms underlying right heart failure: the missing upregulation of superoxide dismutase-2 and its decisive role in antioxidative defense. *Antioxid Redox Signal* 2015;**23**:1220–1332.
12. Pak O, Sommer N, Hoeres T, Bakr A, Waisbrod S, Sydykov A, Haag D, Esfandiary A, Kojonazarov B, Veit F, Fuchs B, Weisel FC, Hecker M, Schermuly RT, Grimminger F, Ghofrani HA, Seeger W, Weissmann N. Mitochondrial hyperpolarization in pulmonary vascular remodeling. *Am J Respir Cell Mol Biol* 2013;**49**:358–367.
13. Pullamsetti SS, Kojonazarov B, Storn S, Gall H, Salazar Y, Wolf J, Weigert A, El-Nikhely N, Ghofrani HA, Krombach GA, Fink L, Gattenlöhner S, Rapp UR, Schermuly RT, Grimminger F, Seeger W, Savai R. Lung cancer-associated pulmonary hypertension: role of microenvironmental inflammation based on tumor cell-immune cell cross talk. *Sci Transl Med* 2017;**9**:eaai9048.
14. Bøtker HE, Hausenloy D, Andreadou I, Antonucci S, Boengler K, Davidson SM, Deshwal S, van Devaux Y, Di Lisa F, Di Sante M, Efentakis P, Femminò S, Garcia-Dorado D, Giricz Z, Ibanez B, Iliodromitis E, Kaludercic N, Kleinbongard P, Neuhäuser M, Ovize M, Pagliaro P, Rahbek-Schmidt M, Ruiz-Meana M, Schlüter K-D, Schulz R, Skyschally A, Wilder C, Yellon DM, Ferdinandy P, Heusch G. Practical guidelines for rigor and reproducibility in preclinical and clinical studies on cardioprotection. *Basic Res Cardiol* 2018;**113**:39.
15. Langer M, Lüttecke D, Schlüter KD. Mechanism of the positive contractile effect of nitric oxide on rat ventricular cardiomyocytes with positive force-frequency relationship. *Pflügers Arch* 2003;**447**:289–297.
16. Wenzel S, Tastan I, Abdallah Y, Schreckenberg R, Schlüter K-D. Aldosterone improves contractile function of adult ventricular cardiomyocytes in a non-acute way: potential relationship to the calcium paradox of aldosteronism. *Basic Res Cardiol* 2010;**105**:247–256.
17. Nippert F, Schreckenberg R, Hess A, Weber M, Schlüter K-D. The effects of swiprosin-1 on the formation of pseudopodia-like structures and β-adrenoceptor coupling in cultured adult rat ventricular cardiomyocytes. *PLoS One* 2016;**11**:e167655.
18. Rupprecht A, Brauer AU, Smorodchenko A, Goyn I, Hilse KE, Shabalina IG, Infante-Duarte C, Pohl EE. Quantification of uncoupling protein 2 reveals its main expression in immune cells and selective up-regulation during T-cell proliferation. *PLoS One* 2012;**7**:e41406.
19. Rupprecht A, Sokolenko EA, Beck V, Ninnemann O, Jaburek M, Trimbuch T, Klishin SS, Jezek P, Skulachev VP, Pohl EE. Role of the transmembrane potential in the membrane proton leak. *Biophys J* 2010;**98**:1503–1511.
20. Gadicherla AK, Wang N, Bulic M, Agullo-Pascual E, Lissoni A, de Smet M, Delmar M, Bultynck G, Krysko DV, Camara A, Schlüter K-D, Schulz R, Kwok W-M, Leybaert L. Mitochondrial Cx43 hemichannels contribute to mitochondrial calcium entry and cell death in the heart. *Basic Res Cardiol* 2017;**112**:27.
21. Boengler K, Bulic M, Schreckenberg R, Schlüter K-D, Schulz R. The gap junction modifier ZP1609 decreases cardiomyocyte hypercontracture following ischaemia/reperfusion independent from mitochondrial connexin 43. *Br J Pharmacol* 2017;**174**:2060–2073.
22. Van der Lee KAJM, Willemsen PHM, van der Vusse GJ, van Bilsen M. Effects of fatty acids on uncoupling protein-2 expression in the rat heart. *FASEB J* 2000;**14**:495–502.
23. Pecqueur C, Alves-Guerra M-C, Gelly C, Levi-Meyrueis C, Couplan E, Collins S, Ricquier D, Bouillaud F, Miroux B. Uncoupling protein 2, *in vivo* distribution, induction upon oxidative stress, and evidence for translational regulation. *J Biol Chem* 2001;**276**:8705–8712.
24. Dando I, Pacchiana R, Pozza ED, Cataldo I, Bruno S, Conti P, Cordani M, Grimaldi A, Butera G, Caraglia M, Scarpa A, Palmieri M, Donadelli M. UCP2 inhibition induces ROS/Akt/mTOR axis: role of GAPDH nuclear translocation in genipin/everolimus anticancer synergism. *Free Radic Biol Med* 2017;**113**:176–189.
25. Anderson KR, Sutton MG, Lie JT. Histopathological types of cardiac fibrosis in myocardial disease. *J Pathol* 1979;**128**:79–85.
26. Mewton N, Liu CY, Croisille P, Bluemke D, Lima JA. Assessment of myocardial fibrosis with cardiovascular magnetic resonance. *J Am Coll Cardiol* 2011;**57**:891–903.
27. Rain S, Andersen S, Najafi A, Schultz JG, da Silva Goncalves D, Handoko ML, Bogaard HJ, Vonk-Noordegraaf A, Andersen A, van der Velden J, Ottenheijm CAC, de Man FS. Right ventricular myocardial stiffness in experimental pulmonary arterial hypertension. *Circ Heart Fail* 2016;**9**:e002636.
28. Mendes-Ferreira P, Santos-Ribeiro D, Adão R, Maia-Rocha C, Mendes-Ferreira M, Sousa-Mendes C, Leite-Moreira AF, Brás-Silva C. Distinct right ventricular remodeling in response to pressure overload in the rat. *Am J Physiol Heart Circ Physiol* 2016;**311**:H85–H95.
29. Vonk Noordegraaf A, Haddad F, Chin KM, Forfia PR, Kawut SM, Lumens J, Naeije R, Newman J, Oudiz RJ, Provencher S, Torbicki A, Voelkel NF, Hassoun PM. Right heart adaptation to pulmonary hypertension. *J Am Coll Cardiol* 2013;**62**:D22–D33.
30. Egemnazarov B, Crnkovic S, Nagy BM, Olschewski H, Kwapiszewska G. Right ventricular fibrosis and dysfunction: actual concepts and common misconceptions. *Matrix Biol* 2018;**68-69**:507–521.

31. Westerhof BE, Saouti N, van der Laarse WJ, Westerhof N, Vonk Noordegraaf A. Treatment strategies for the right heart in pulmonary hypertension. *Cardiovasc Res* 2017;**113**:1465–1473.
32. Cartledge JE, Kane C, Dias P, Tesfom M, Clarke L, Mckee B, Al Ayoubi S, Chester A, Yacoub MH, Camelliti P, Terracciano CM. Functional crosstalk between cardiac fibroblasts and adult cardiomyocytes by soluble mediators. *Cardiovasc Res* 2015;**105**: 260–270.
33. Cheng TC, Philip JL, Tabima DM, Hacker TA, Chesler NC. Multiscale structure-function relationships in right ventricular failure due to pressure overload. *Am J Physiol Heart Circ Physiol* 2018;**315**:H699–H708.
34. Turner JD, Gaspers LD, Wang G, Thomas AP. Uncoupling protein-2 modulates myocardial excitation-contraction coupling. *Circ Res* 2010;**106**:730–738.
35. Moon MR, Aziz A, Lee AM, Moon CJ, Okada S, Kanter EM, Yamada KA. Differential calcium handling in two canine models of right ventricular pressure overload. *J Surg Res* 2012;**178**:554–562.